

Short Communication

Surface Modification of Titanium by Hydroxyapatite/CaSiO₃/Chitosan Porous Bioceramic Coating

Lan Zhang

Department of Pharmacy, Xiamen Medical College, Xiamen 361023, Fujian, China
E-mail: zhanglan7578@163.com

Received: 6 June 2019 / Accepted: 8 January 2020 / Published: 10 March 2020

In this study, hydroxyapatite(HA)-CaSiO₃-chitosan(CS) composite bioceramic coating was applied to the surfaces of pure titanium by using the electrophoretic deposition (EPD) method. The mechanism of EPD of HA/CaSiO₃/CS composites is discussed. The composite bioceramic coating was followed by heat treatments in a controlled atmosphere to make coatings porous and enhance their mechanical properties due to CS and CaSiO₃ particles. The composition, structure, and surface morphology of these coatings are characterized through fourier transform infrared spectroscopy(FTIR), X-ray diffraction(XRD), field emission scanning electron microscopy(SEM) and transmission electron microscope(TEM). Our results confirmed that this approach is especially attractive for the fabrication of porous bioceramic coatings. The adhesive force between the HA/CaSiO₃ porous coatings and pure titanium is approximately 26.6 MPa. The porous HA/CaSiO₃ coatings provide improved bioactivity and biocompatibility of pure titanium in the simulated body fluid solution.

Keywords: Electrophoretic deposition, hydroxyapatite, chitosan, CaSiO₃, porous coatings, surface modification.

1. INTRODUCTION

Various methods have been studied to improve the bioactivity of titanium implants. Among them, electrophoretic deposition (EPD) is an effective method for the processing of bioactive coatings onto titanium implants, specifically hydroxyapatite coatings[1][2][3].

Hydroxyapatite [Ca₁₀(PO₄)₆(OH)₂] (HA) represents about 70% similar to natural human bones, it has been widely applied in orthopedics[3]. Therefore, poor mechanical strength of HA coating to the titanium substrate is to be expected. To solve this problem of HA bioceramic coatings, one solution to this problem is the deposition of HA/CaSiO₃ composite coating on titanium implants. The bioactivity of CaSiO₃ is high due to the fast resorption an apatite layer on its surface after in biological environments[4]. In addition, CaSiO₃ as intermediate particles could adhere tightly to HA and titanium substrate after sinter[5].

Porous ceramic materials have been investigated in several fields such as biomaterials. Recently, porous ceramic materials with highly controlled porous structures have been fabricated by forming pore agents method using polymer particles as pore-forming agent(PFA)[6]. Among PFAs, chitosan(CS) is an important one. CS exhibits excellent properties such as biocompatibility, chemical, stability[7]. The pore agents process mainly consists of three steps: the first one is a formation of HA suspensions containing CaSiO_3 and CS particles, the second is a formation of HA/ CaSiO_3 /CS composite coating onto titanium by EPD, the last one is a remove of the PFA by either heat treatment.

In this report, porous HA/ CaSiO_3 bioceramic coating was prepared by the EPD process, bond-pull strength tests have been carried out to measure the mechanical property of the coating, in vitro biocompatibility for the porous bioceramic coating was soaked in simulated body fluid (SBF) bath.

2. MATERIALS AND METHODS

Pure titanium (Ti) discs were etched in 5% hydrofluoric acid and 5 mol/L nitric acid, followed by washing in acetone in an ultrasonic bath for 30 min. CS with a degree of deacetylation of about 96.4% was purchased from Qingdao Jinhua Co. Ltd. . CaSiO_3 , $\text{Ca}(\text{NO}_3)_2$, $\text{NH}_4\text{H}_2\text{PO}_4$ and polyethylene glycol was purchased from Shanghai Chemical Reagent Corporation.

2.1. Hydrothermal synthesis of HA powders

Hydrothermal method was applied to prepare HA powders. First, analytically pure $\text{Ca}(\text{NO}_3)_2$ and $\text{NH}_4\text{H}_2\text{PO}_4$ were dissolved in deionized water to form 0.5 and 0.3 M aqueous solutions, respectively. 0.2wt.% polyethylene glycol as the dispersant dissolved in $\text{Ca}(\text{NO}_3)_2$ solution. These two aqueous solutions were separately adjusted to pH=10 using ammonium hydroxide. The $\text{NH}_4\text{H}_2\text{PO}_4$ solution was added to $\text{Ca}(\text{NO}_3)_2$ suspension drop by drop at room temperature under magnetic stirring. Then, the reaction product was poured into an autoclave with Teflon inner liner and aged for 10 h at 200°C . Finally, the resulting white precipitate was filtered, washed thoroughly with distilled water and oven-dried at about 100°C for 2h[8].

2.2. Suspension preparation and EPD

Table 1 shows ingredients of suspensions for fabrication of HA/ CaSiO_3 /CS composite coating. HA, CS and CaSiO_3 particles(m/m/m)were added to 40 mL n-butanol with $12\text{ mL}\cdot\text{L}^{-1}$ dispersant referred to the n-butanol and then dispersed in ultrasonic bath for 60 min. The suspensions were then allowed to settle for 24 hours[9].

Table 1. Ingredients of suspensions for fabrication of HA/CaSiO₃/CS composite coating via electrophoretic deposition (EPD)

Suspension	HA / g	CaSiO ₃ / g	CS / g
HA/CaSiO ₃ /CS-S1	0.268	0.268	0.268
HA/CaSiO ₃ /CS-S2	0.400	0.240	0.160
HA/CaSiO ₃ /CS-S3	0.400	0.160	0.240

Cathodic deposits were obtained on Ti(10×10×1 mm) connected to an electrophoresis apparatus (Beijing Liuyi Instrument Factory, China). The distance between the cathode and anode was 10 mm. The current density was 0.1 mA/cm². Fig. 1 shows the electrochemical cell for the deposition. The coatings were dried at 40 °C values for 8h and then sintered in a muffle furnace at 700°C for 2 h in an air atmosphere. Thus, the obtained porous coatings were immersed in a 1.5 simulated body fluid(1.5 SBF) with pH=7.4 at 37 °C for 7 days. An aqueous solution(1.5 SBF) contains 1.5 times higher concentrations of inorganic ions than human body plasma, as shown in Table 2[10], which was used to accelerate the apatite formation of the coating surface. The solution was prepared by dissolving the reagents of NaCl, KCl, MgCl₂·6H₂O, CaCl₂, NaHCO₃, K₂HPO₄·3H₂O and Na₂SO₄ into distilled water[11].

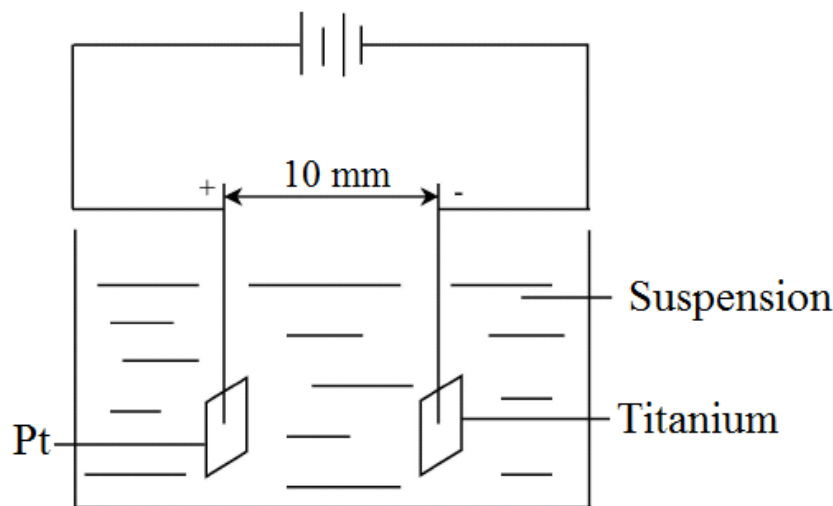


Figure 1. The electrophoretic deposition apparatus.

Table 2. The ion concentration of simulated body fluid and body plasma

Ions	Na ⁺	K ⁺	Mg ²⁺	Ca ²⁺	Cl ⁻	HCO ₃ ⁻	HPO ₄ ²⁻	SO ₄ ²⁻
Human plasma (mmol/L)	142.0	5.0	1.5	2.5	103.0	27.0	1.0	0.5
SBF (mmol/L)	142.0	5.0	1.5	2.5	148.8	4.2	1.0	0.5
1.5 SBF (mmol/L)	213.0	7.5	2.3	3.8	223..2	6.3	1.5	0.75

2.3. Coating characterization

The phase content of porous coatings were investigated by the A Philips X'Pert MPD X-ray diffractometer system (XRD). A Fourier transform infrared spectroscopy (FTIR) was used to study chemical content of HA. CS and composite coatings. A JEOL 7500F Field Emission Scanning Electron Microscope (FESEM) and JEOL 2010F Transmission Electron Microscope (TEM) were used to observe size and morphology of the precipitated HA particles and HA coating respectively. The adhesive strength between the Ti substrate and composite coating were tested according to ASTM F1044-87, which was carried out with a universal testing machine (Model LR5K, Lloyd Ltd. UK). A CHI660C potentiostat was used to observe protective properties of the composite coatings in 1.5SBF solution. A conventional three-electrode cell was utilized, the composite coating was used as working electrode, with a platinum mesh being the counter electrode and a saturated calomel electrode (SCE) as the reference electrode respectively. The potentiodynamic polarization curves was recorded from -0.4 V to 0.2 V with a scanning rate of 1 mV/s. The EIS measurements were performed at open circuit potential with a frequency range of 10 mHz–100kHz.

3. RESULTS AND DISCUSSION

Fig. 2 shows the XRD pattern of HA powders prepared by hydrothermal method. The XRD pattern indicates that diffraction peaks of coating are similar to HA crystals according to JCPDS 09-432.

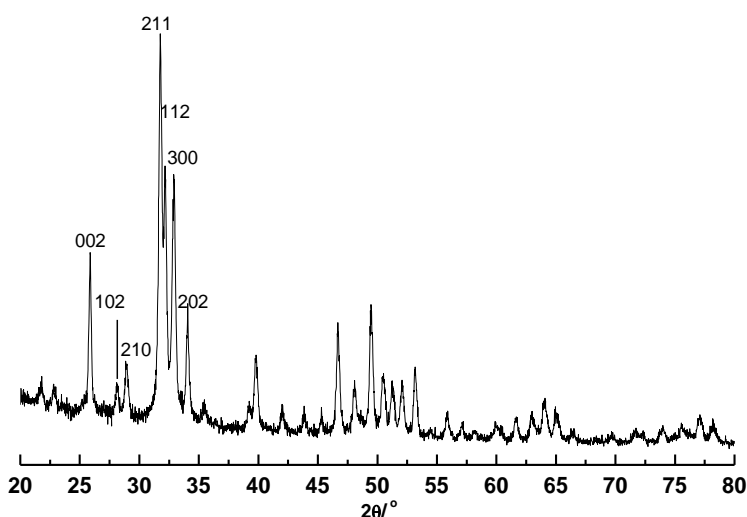


Figure 2. X-ray diffraction (XRD) patterns of HA nano-particles

Fig. 3 shows the TEM micrographs of HA powder by hydrothermal method. It is can be that rod-like nano-particles were successfully fabricated with a length of about 10-200 nm and a diameter of about 5-20 nm.

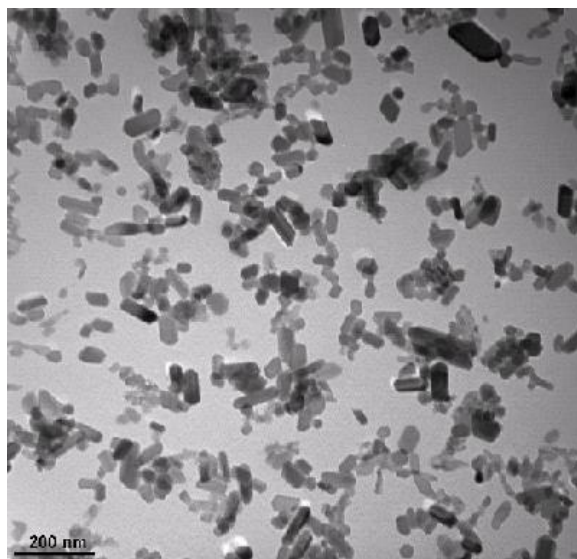


Figure 3. TEM image of the HA nanoparticles

Fig. 4 shows the FTIR spectrum of different coating samples. The stretching mode of hydroxyl presents a broad peak around at 3571cm^{-1} . The stretching mode of chitosan C=O (amide I) group occur at 1638cm^{-1} . The peak at 1598cm^{-1} related to bending mode of $-\text{NH}_2$ group of chitosan. The stretching mode of $-\text{C}-\text{O}-$ appears at 1385cm^{-1} is related to $-\text{CH}_2-\text{OH}$ group of chitosan[12]. The peaks in the region $550\sim 700\text{cm}^{-1}$ and $880\sim 1100\text{cm}^{-1}$ corresponding to $\beta\text{-CaSiO}_3$ [13]. Also the peaks at 1067 , 1021 , 646 , and 565cm^{-1} can be attributed to phosphate groups of HA. The results of FTIR spectrum indicate the fabrication of HA coatings containing CS, CaSiO_3 particles. Fig. 5 shows the XRD pattern of the electrophoretically fabricated coatings were heated with temperatures $700\text{ }^\circ\text{C}$ for 2 h in air atmosphere. The XRD pattern indicates that diffraction peaks of coating are similar to HA and CaSiO_3 (imaginary line) crystals according to JCPD 10-0486.

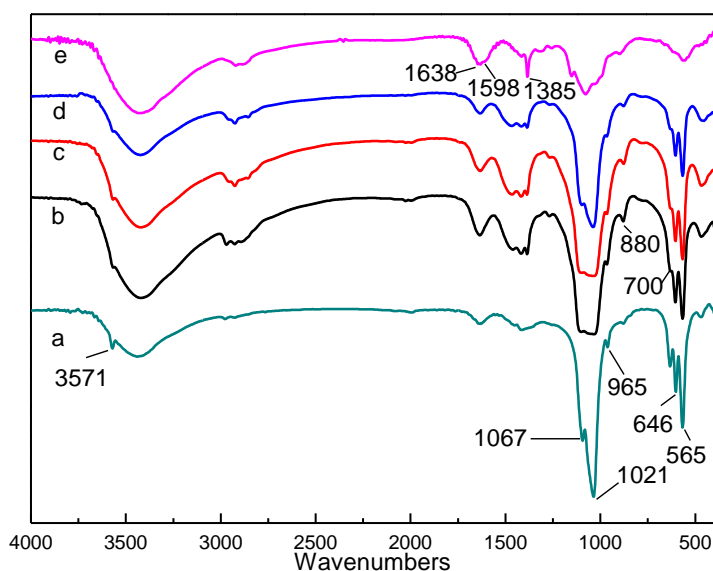


Figure 4. FT-IR spectra of (a): pure HA, (b): HA/ CaSiO_3 /CS-S1, (c): HA/ CaSiO_3 /CS-S2, (d): HA/ CaSiO_3 /CS-S3, (e): pure CS

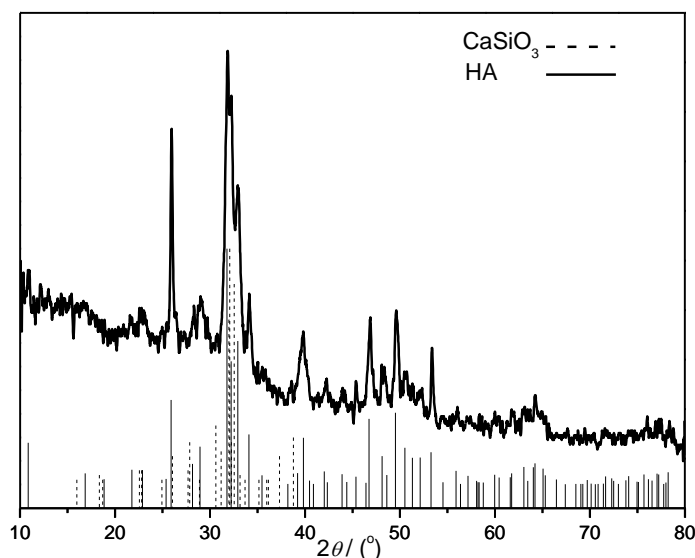
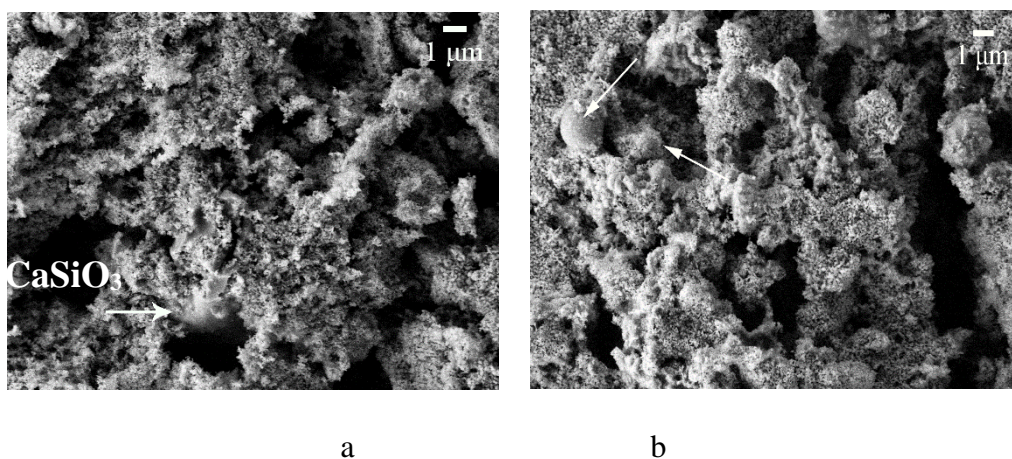


Figure 5. X-ray diffraction (XRD) patterns of HA/CaSiO₃ composite coatings

As mentioned, The results clearly suggest that HA, CaSiO₃ and CS particles became positively charged in contact with n-butanol, moving toward the cathode(substrate) electrode and were deposited there only[14]. SEM micrographs of the electrophoretically fabricated coatings are shown in Figure 6, which were heated with temperatures 700 °C for 2 hours in atmosphere. As can be seen in Fig.6, the macropores in the coating layer were produced from the co-deposition of CS by the heat treatment, average pore diameter of 5~10 μm (Fig.6 c, d) was obtained when using 38.5 μm size CS, the average pore size of the coatings slightly reduced which could be due to post-sintering of HA nanoparticles[15]. Fig. 6 (a, b) graphs show the co-deposition of ceramic materials, which covered the surface of the CaSiO₃ particles. Fig. 7 shows the cross-sectional morphologies between the ceramic layer and substrate, the effect of the CaSiO₃ particles as possible reinforcement element in the sintered laminate composite remains to be investigated.



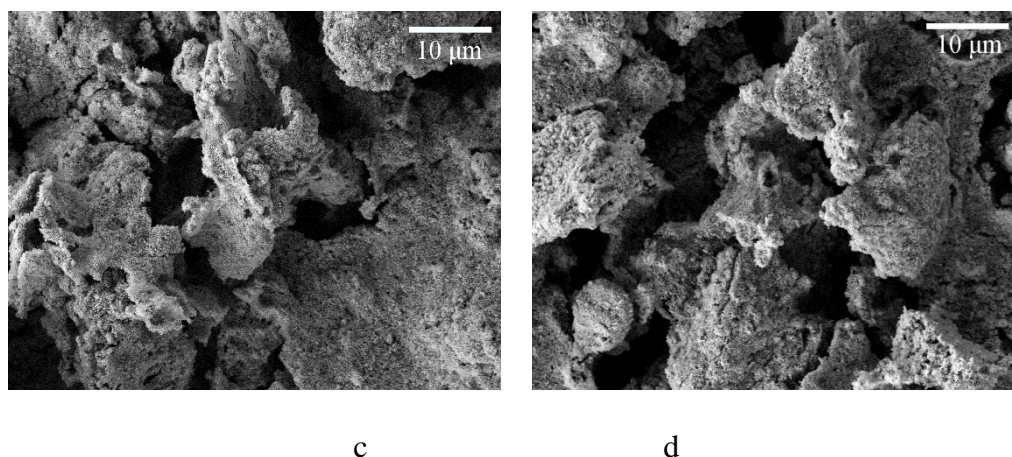


Figure 6. SEM pictures of the HA-chitosan composite coatings prepared from the n-butanol solutions containing HA , CS and CaSiO₃ (a, b), and (c, d) at different magnifications by sintering at 700°C for 2 h

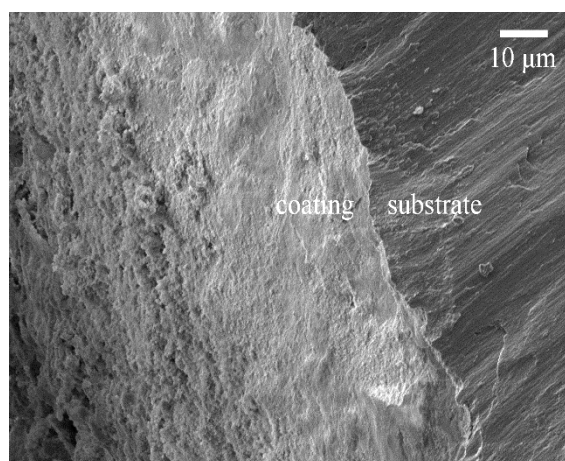


Figure 7. SEM photographs of cross-sectional morphologies of HA/CaSiO₃/CS composite coating after heat treatment at 700°C

The mechanical properties of CaSiO₃ particles additions on electrophoretically formed coating layers were measured by shear strength tests after samples sintered at 700°C for 2 h under flowing air atmosphere. The results were presented in Table 3 that bonding strength values of coating layer and substrate increase with increasing amount of CaSiO₃, porous HA/CaSiO₃ coating obtained using HA/CaSiO₃/CS-S1 suspension has bonding strength values upto 26.6 MPa, the bonding strength between coating and Ti implant is highly important issue of the replaced implant in life cycle[16].

Table 3. The effects of CaSiO₃ on the mechanical properties of EPD-formed coating layers after sintering at 700°C for 2 h under flowing air

Suspension	HA/CaSiO ₃ /CS-S1	HA/CaSiO ₃ /CS-S2	HA/CaSiO ₃ /CS-S3
Bonding strength σ (MPa)	26.6	26.2	24.4

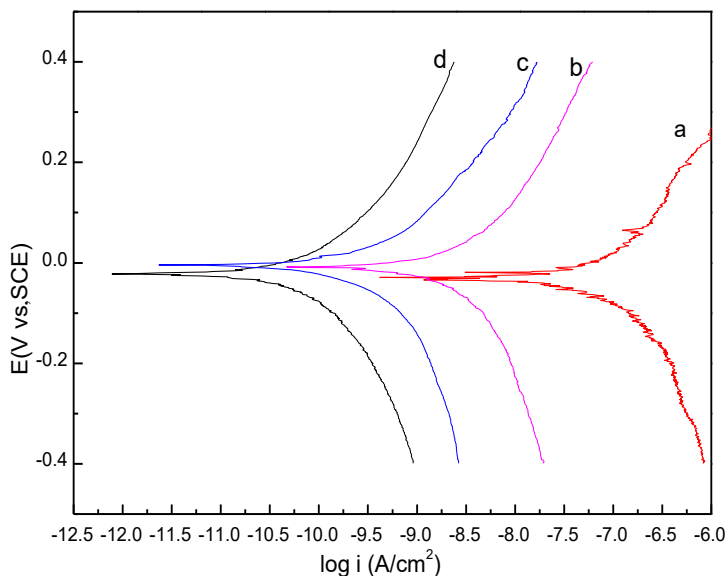


Figure 8. Potentiodynamic curves of uncoated (a: Pure titanium) and (b: HA/CaSiO₃/CS-S1, c: HA/CaSiO₃/CS-S2, d: HA/CaSiO₃/CS-S3) the coated titanium samples in the SBF solution and heat treated at 700 °C for 2 h.

Table 4. Electrochemical parameters for (a) pure titanium and (b: HA/CaSiO₃/CS-S1, c: HA/CaSiO₃/CS-S2, d: HA/CaSiO₃/CS-S3) porous HA/CaSiO₃ coatings in 1.5SBF

Sample	E _{corr.} (V)	I _{corr.} (10 ⁻⁸ A)
Ti	-0.0236	6.792
HA/CaSiO ₃ /CS-S1	-0.0093	0.228
HA/CaSiO ₃ /CS-S2	-0.0178	0.026
HA/CaSiO ₃ /CS-S3	-0.0207	0.007

The electrochemical behavior of uncoated and coated Ti samples immersed in the 1.5 SBF solution were compared in Fig. 8. The corrosion current(I_{corr.}) and corrosion potential(E_{corr.}) were obtained from the Tafel extrapolation of anodic and cathodic region and was displayed in Table 4. From the I_{corr.} values with HA/CaSiO₃ and have shown less corrosion current density than pure titanium, due to the coated HA and CaSiO₃ particles after heat treated at 700 °C, there by leads to dense coating on the titanium surface[17]. Such an equivalent circuit was previously reported as obtained by simulation from the fitting of the EIS Nyquist plot used in studying the ionic conductivity in films and consists of one resistor(R₂), one electrolyte resistance(R₁) and one capacitor(C_d) in parallel[18](Fig. 9a). Further on, the experimental fact of a single semi-circle evidences conditions of good corrosion resistance of prepared coating to the Ti surface (Fig. 9b). Fig.10 shows the impedance data of coated samples. It can be seen that the impedance values of coated samples were increased compared to the uncoated sample, and the heat treatment of coated samples resulted in a further increase in the impedance[19].

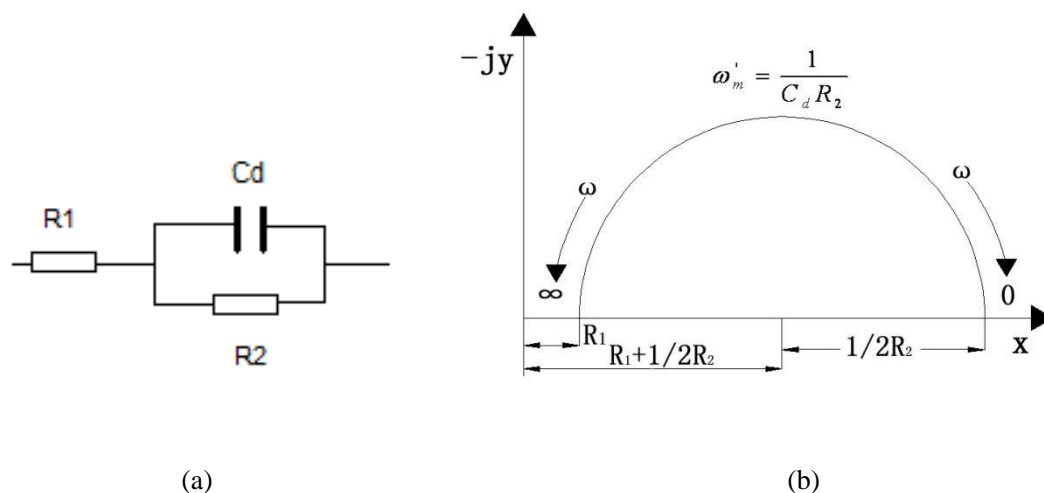


Figure 9. (a) Electrochemical polarization equivalent circuit of the electrode, (b) The Nyquist plot of equivalent circuit

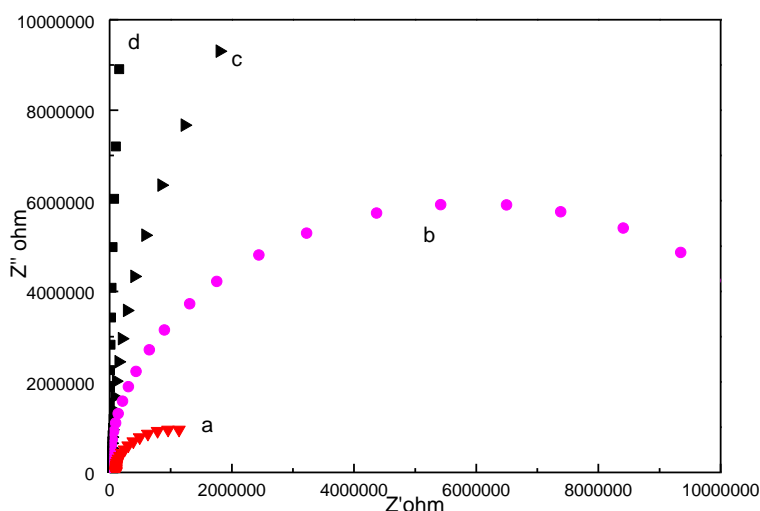


Figure 10. The Nyquist plots of pure titanium and porous HA/CaSiO₃ coatings in SBF (a: Pure titanium, b: HA/CaSiO₃/CS-S1, c: HA/CaSiO₃/CS-S2, d: HA/CaSiO₃/CS-S3)

Fig. 11 shows the SEM micrograph of the top surfaces of porous HA/CaSiO₃ coating onto the substrate after soaking in 1.5SBF for some days, these micrographs indicated that bonelike apatite crystals overgrew on whole coating surface and macropores. This crystal growth rate of porous HA/CaSiO₃ coating was higher than that of a dense hydroxyapatite coating prepared by the EPD method too[20]. This improvement of in vitro biocompatibility is changed by the formation of macropores and CaSiO₃.

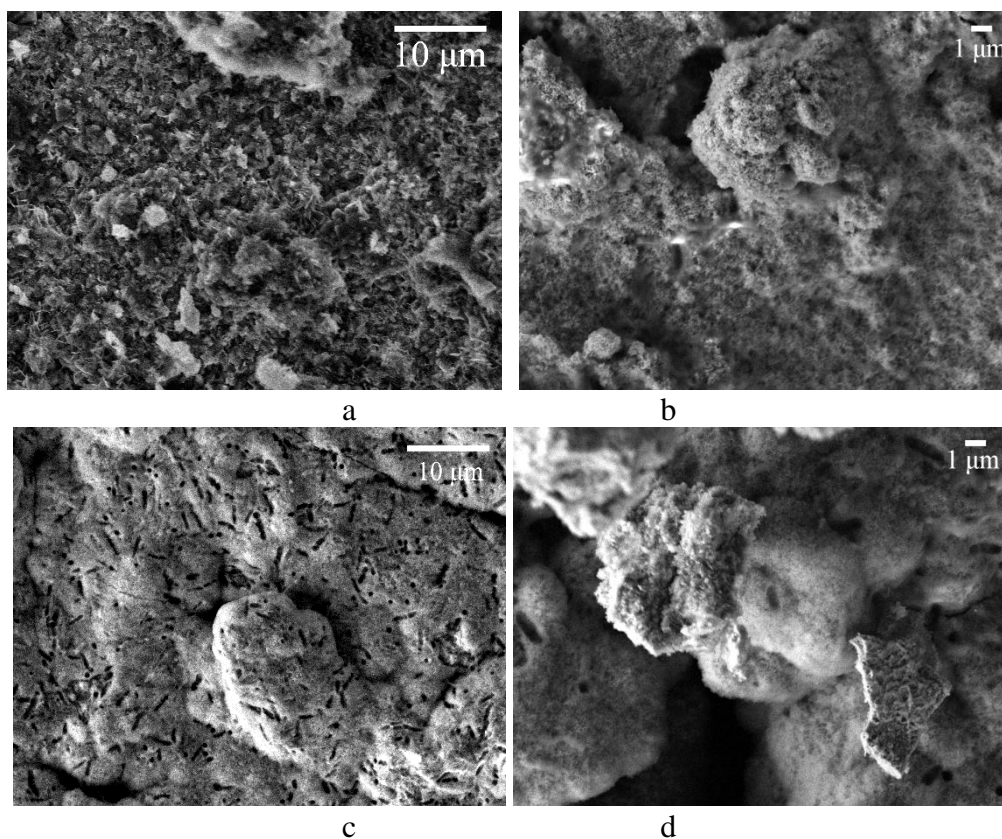


Figure 11. Surface morphologies of without pores(a, b) and porous HA/CaSiO₃ coatings after soaking in a simulated body fluid at 37 °C for 7 d (c, d)

4. CONCLUSION

Novel HA/CaSiO₃/CS composite coatings have been prepared using electrophoretic deposition technique. The porous HA/CaSiO₃ coatings were obtained as average pore diameter of 5~10 μm after the heat treatments with temperatures 700 °C for 2 hours in atmosphere. The adhesive force between the HA/CaSiO₃ porous coatings and pure titanium is approximately 26.6 MPa. The porous HA/CaSiO₃ coatings provide improved bioactivity and biocompatibility of pure titanium through soaking in the 1.5SBF solution at 37 °C for 7 days. Furthermore, the EIS data demonstrated that the obtained porous composite coatings act as a protective layer and improve the corrosion resistance of the Ti substrates.

References

1. R. M. Kumar, K. K. Kuntal, S. Singh, P. Gupta, B. Bhushan, P. Gopinath, D. Lahiri, *Surf. Coat. Technol.*, 287 (2016) 82.
2. M. Farrokhi-Rad, T. Shahrabi, S. Mahmoodi, Sh. Khanmohammadi, *Ceram. Int.*, 43 (2017) 4663.
3. R. Drevet, N. B. Jaber, J. Fauré, A. Tara, A. B. C. Larbi, H. Benhayoune, *Surf. Coat. Technol.*, 301 (2016) 94.
4. A. Pawlik, M. A. U. Rehman, Q. Nawaz, F. E. Bastan, G. D. Sulka, A. R. Boccaccini, *Electrochim. Acta*, 307 (2019) 465.

5. D. Zhitomirsky, J. A. Roether, A. R. Boccaccini, I. Zhitomirsky, *J. Mater. Process. Technol.*, 209 (2009) 1853.
6. A. K. Gain, L. C. Zhang, W. D. Liu, *Mater. Des.*, 67 (2015) 136.
7. F. Sun, X. Pang, I. Zhitomirsky, *J. Mater. Process. Technol.*, 3 (2009) 1597.
8. X. F. Xiao, R. F. Liu, *Mater. Let.*, 60 (2006) 2627.
9. M. Farrokhi-Rad, T. Shahrabi, *Ceram. Int.*, 39 (2013) 3031.
10. M. Tanahashi, T. Yao, T. Kokubo, *J. Am. Ceram. Soc.*, 77 (1994) 2805.
11. T. Kokubo, K. Hata, T. Nakamura, T. Yamamuro, *Biomaterials*, 4 (1991) 113.
12. R. Murugan, S. Ramakrishna, *Biomaterials*, 25 (2004) 3829.
13. X. Pang, T. Casagrande, I. Zhitomirsky, *J. Colloid. Interf. Sci.*, 330 (2009) 323.
14. X. Pang, I. Zhitomirsky, *Mater. Chem. Phys.*, 94 (2005) 245.
15. H. Jun-ichi, A. Yuki, K. Kiyoshi, *J. Ceram. Soc. Jpn.*, 114 (2006) 51.
16. M. Wei, A. J. Ruys, B. K. Milthorpe, C. C. Sorrell, J. H. Evans, *J. Sol-gel Sci. Technol.*, 21 (2001) 39.
17. M.E. Escalante-Perez, J. Porcayo-Calderon, E. Vazquez-Velez, *Int. J. Electrochem. Sci.*, 11 (2016) 374.
18. C. Amaya, W. Aperador, J.C. Caicedo, F.J. Espinoza-Beltrán, J. Muñoz-Saldaña, G. Zambrano, P. Prieto, *Corros. Sci.*, 51 (2009) 2994.
19. C. T. Kwok, P. K. Wong, F. T. Cheng, *Appl. Surf. Sci.*, 255 (2009) 6736.
20. J. Hamagami, Y. Ato, K. Kanamura, *Solid State Ion.*, 172 (2004) 331.

© 2020 The Authors. Published by ESG (www.electrochemsci.org). This article is an open access article distributed under the terms and conditions of the Creative Commons Attribution license (<http://creativecommons.org/licenses/by/4.0/>).